

THE EFFECT OF MULTIPLE ALTERATION PROCESSES ON SKYROS CHROMITITES (NORTHERN SPORADES, GREECE)

Micol Bussolesi^{*,✉}, Giovanni Grieco^{**}, Federica Zaccarini^{***}, Fahui Xiong[°] and Alessandro Cavallo^{*}

* Department of Earth and Environmental Sciences, University of Milano-Bicocca, Milano, Italy.

** Department of Earth Sciences, University of Milano, Italy.

*** Geosciences Programme, Faculty of Science, Universiti Brunei Darussalam, Jalan Tungku Link, Gadong, Brunei Darussalam.

° Key Laboratory of Deep-Earth Dynamics of Ministry of Natural Resources, Institute of Geology, Chinese Academy of Geological Sciences, China.

✉ Corresponding author, e-mail: micol.bussolesi@gmail.com

Keywords: chromitites; ophiolites; Cr-garnets; Skyros Island.

ABSTRACT

Skyros Island, in the Aegean Sea, hosts significant mafic-ultramafic bodies scattered within the subophiolitic mélangé. Small chromite deposits crop out in three close localities, Northern Agios Iohannis, Agios Iohannis and Agia Alexandria. Chromitites and their host rocks are heavily altered and display an uncommon mineral assemblage. Primary minerals include orthopyroxene and clinopyroxene relics along with unaltered chromite. Northern Agios Iohannis spinels have average $Cr\# = Cr/(Cr + Al)$ of 0.74, compatible with a boninitic parental melt, while Agios Iohannis and Agia Alexandria have lower $Cr\#$ (0.65-0.68), compatible with a MORB-like parental melt. Considering the proximity of the three localities, the changes in mineral chemistry can be due to: i) Genesis of the chromite pods in different dunite channels, from different parental magmas. ii) Evolution from MORB-like to boninitic melts during subduction. iii) Melt/rock interactions with variably depleted peridotite sources; iv) Genesis of the chromitites in compositionally different mantle slices, tectonically dismembered and juxtaposed. Three alteration events were detected: i) serpentinization, with replacement of primary silicates by serpentine (widespread at Agios Iohannis and Northern Agios Iohannis and more limited at Agia Alexandria); ii) chloritization, involving a reaction of chromite and serpentine with oxidizing fluids to form Fe-chromite and chlorite; iii) reaction of Fe-chromite and serpentine to form Cr-garnets with a composition lying in the uvarovite-andradite solid solution (at Agios Iohannis and Northern Agios Iohannis, absent at Agia Alexandria). Despite the restricted geographical area, the three localities display heterogeneity in the primary and secondary features, highlighting compositional variation of the parent melt and local changes in fO_2 and fS_2 during the alteration events. The order in which the alteration events occur in an ophiolite can strongly affect the final mineral assemblage. Cr-garnets can be Fe- or Al-rich based on the magnitude and order of previous alteration stages. In particular, chloritization events lead to loss in Al in the spinel, so the garnet forming reaction will lead towards uvarovite-andradite solid solution products.

INTRODUCTION

Ophiolites can host important chromite deposits, scattered in the mantle section and ultramafic cumulates above the Moho. These deposits form pods and lenses of variable thickness and are economically renowned for the high quality of chromite for the metallurgical industry (Schulte and Pack, 2024).

According to published genetical models, the majority of podiform chromitites is generated in Supra-Subduction Settings (SSZ), when melts with different composition mix within restitic dunite channels, shifting the composition in the chromite stability field (Spiegelman and Kelemen, 2003; González-Jiménez et al., 2014; Cocomazzi et al., 2020). Other authors suggest instead that this genetical model is inadequate to explain the formation of chromitites, and that podiform deposits are the result of extensive melt/rock reaction in the upper mantle (Zhou and Robinson, 1994; Arai, 1997; Zhou et al., 2001;)

Cr-spinel compositions within ophiolite chromitites can be highly variable, from high-Cr to high-Al, depending on their tectonic setting (e.g., forearc, backarc), and their geochemical affinity (e.g., forearc, backarc and mid-ocean ridge) (Dilek and Furnes, 2014). High-Cr chromitites are generally thought to have formed from boninitic magmas (Abe, 2011; Dick and Bullen, 1984; Zhou et al., 1996), whereas Cr-poor chromitites are believed to be generated from MORB-like or arc tholeiite magmas (Dick and Bullen, 1984; Melcher et

al., 1997). Bimodal occurrences of Cr-rich and Cr-poor chromitites in the same ophiolitic complex have been interpreted as an evolution from a MORB-like parental melt to a boninitic one at subduction initiation (Uysal et al., 2016; Qiu et al., 2018; Chen et al., 2019; Bussolesi et al., 2022a).

Podiform chromitites are generally subject to a complex post-magmatic history involving the circulation of fluids and replacement of primary minerals with secondary ones. The most common alteration processes are serpentinization (Frost and Beard, 2007; Grieco and Merlini, 2012; Liu et al., 2023) and chloritization (Proenza et al., 1999; Bussolesi et al., 2022b), which completely replace primary silicates with serpentine and chlorite. Chromite is also affected by these post-magmatic processes by progressively losing Al and Cr, thus transforming into ferrian-chromite and, in the most extreme cases, into Cr-magnetite (Mellini et al., 2005; Saumur and Hattori, 2013; Ahmed and Surour, 2016). Finally, the Base Metals and Platinum Group Elements sulfides are also heavily affected by serpentinization processes, which cause remobilization of the metals and in some cases desulfurization and transformation into alloys (Zaccarini et al. 2005; Proenza et al., 2007; Tsoupas and Economou-Eliopoulos, 2008; Grieco et al., 2020).

The present contribution aims to provide new insights into the magmatic and post-magmatic evolution of Skyros podiform chromitites, and to provide new interpretations for the formation of unusual mineral assemblages during chromitites alteration processes.

GEOLOGICAL BACKGROUND

Skyros is the largest island of the Northern Sporades Archipelago, located in the Aegean Sea. Geologically, it is part of the Albanide-Hellenide orogenic belt, subdivided into three tectono-stratigraphic domains (Fig. 1) (Chiari et al., 2012; Bortolotti et al., 2013; Saccani et al., 2008; 2015; 2017). From W to E, they are the Adria Continental, the Vardar, and the Serbo-Macedonian Rhodope Domains (Bortolotti and Principi, 2005; Ferrière et al., 2012; Bortolotti et al., 2013). The Adria Continental Domain, comprising tectonic units originated from the Eastern continental margin of the Adria Plate, includes the Pelagonian and Subpelagonian zones (Chiari et al., 2012; Saccani et al., 2015). The Vardar Domain represents an oceanic suture zone and is divided into three sub-zones: the Almopias (oceanic), Paikon (continental), and Peonias/Guevgueli (oceanic) (Saccani et al., 2008; 2015; Ferrière et al., 2012). Finally, the Serbo-Macedonian Rhodope Domain represents the Eastern margin of the Eurasia Plate. Several ophiolites crop out in the Albanide-Hellenide Belt. (Saccani et al., (2011) grouped them into i. External (or Western) Ophiolites (part of the Pelagonian and Subpelagonian Zones); ii. Internal (or Eastern) Ophiolites (part of the Vardar Domain). The External Ophiolites consist of Triassic-Jurassic ophiolite sequences generated both in oceanic (MOR) and supra-subduction zone (SSZ) settings (Beccaluva et al., 1994; Saccani et al., 2011). The Internal Ophiolites are characterized by Jurassic and subordinate Triassic ophiolitic units and related sedimentary covers (Almopias subzone), Middle to Upper Jurassic sequences formed in an arc setting (Paikon subzone), and Middle-Upper Jurassic ensialic back-arc sequences (Peonias/Guevgueli subzone) (Saccani et al., 2008; 2011; 2015). Ophiolites cropping out within the Serbo-Macedonian Rhodope Massif (Therma-Volvi-Gomati complex) have still an unclear origin, and represent either a remnant of the Permian Palothetys Ocean or a Middle Triassic rift-related magmatic suite (Bonev et al., 2019).

The geology of Skyros is quite complex. The island is tec-

tonically included in the Pelagonian - Subpelagonian Zones of the Adria domain, and the main geological units are, from bottom to the top (Karkalis et al., 2017; Boundi et al., 2024):

i - Sub-Pelagonian Unit, making up the Southern and North-Western part of the island, comprising a Triassic-Jurassic carbonate platform.

ii- Ophiolites of the Vardar Domain, tectonically emplaced onto the carbonate platform (formerly addressed to as "Eohellenic Nappe").

iii- Pelagonian Zone, comprising Late Cretaceous Limestones and Flysch.

iv- Lower Metamorphic Unit of Skyros, comprising meta-volcanic rocks, meta-sediments, and pelagic silicate marbles.

v- Upper Metamorphic Unit of Skyros, comprising pelagic silicate marbles and intercalations of gneisses-schists.

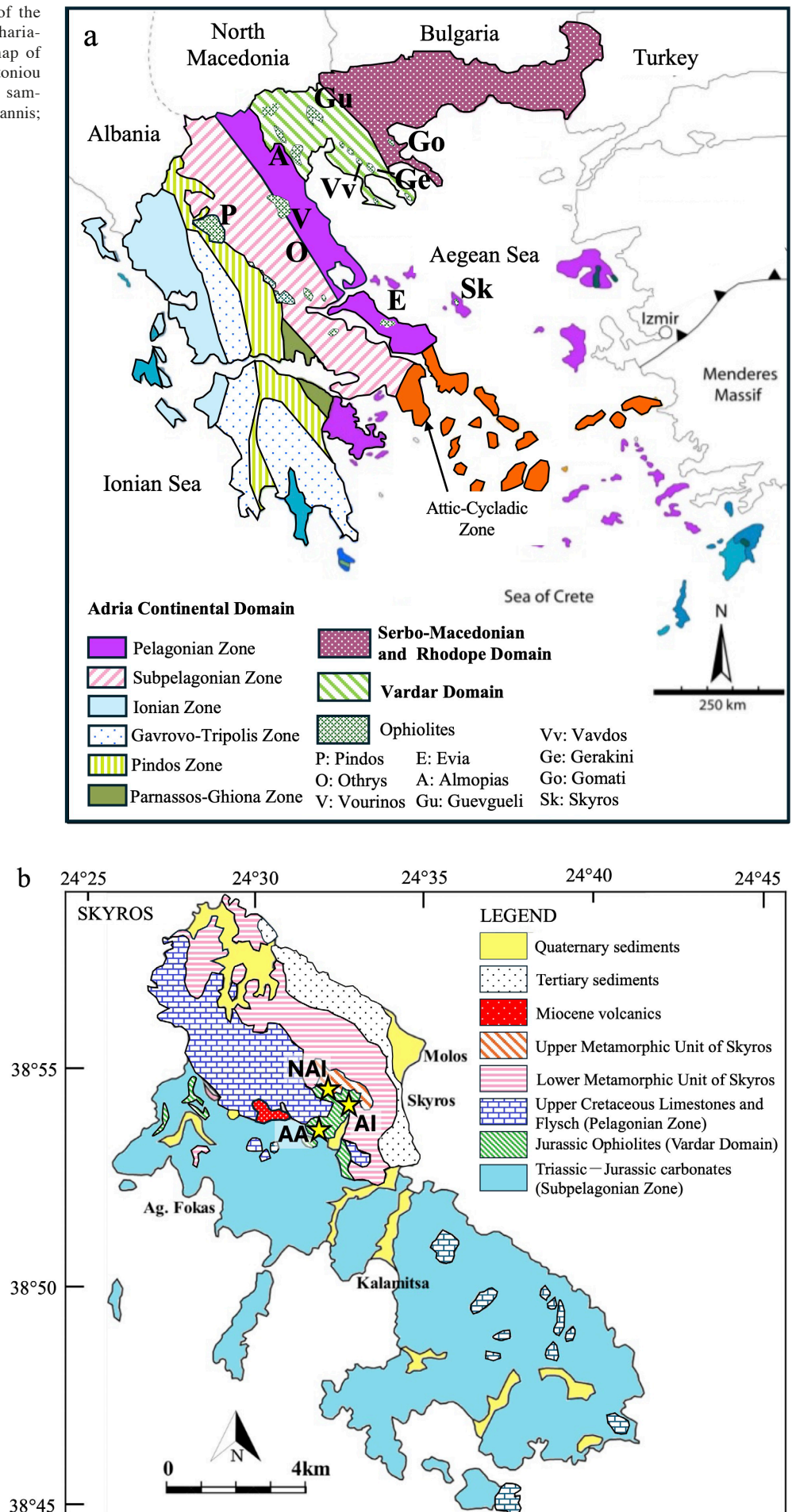
The Northern part of the island is additionally covered by Tertiary and Quaternary sediments, and Miocene Volcanics crop out in the central area of NW Skyros (Karkalis et al., 2017) (Fig. 1b). (Beccaluva et al., 1994; Robertson et al., 1996; Rassios and Dilek, 2009) (Kilias et al., 2010; Schmid et al., 2008). Skyros ophiolites, are represented by the sub-ophiolitic mélange of the Vardar Domain, which includes highly deformed serpentinites, Triassic volcanic and sedimentary rocks, basalts and radiolarian cherts of both Triassic and Jurassic ages (Saccani and Photiades, 2005; Karkalis et al., 2017). The ophiolites were emplaced during Late Jurassic to Early Cretaceous, and tectonically overthrust the Pelagonian zone rocks (Harder et al., 1983; Pe-Piper and Piper, 2002, Boundi et al., 2024).

Ultramafic bodies in Skyros consist of serpentinitized dunites and harzburgites. Small chromitite and magnetitite lenses are scattered into the dunites, forming sub-economic bodies (Karkalis et al., 2017). A carbonation event is testified by the presence of rodingite dykes, rich in hydrogarnets, vesuvianite, chlorite, diopside, and clinopyroxene. The high levels of serpentinitization and rodingitization reflect alteration processes that affected the Skyros ultramafic massif during exhumation, due to circulation of hydrothermal fluids, possibly generated during subduction (Karkalis et al., 2017).

Table 1- Skyros samples and coordinates.

Area	Coordinates	Sample	Lithology
	38°54'05.45'' – 24°32'48.21''	Sky8a, Sky8b, Sky8c	Chromitite
Agios Iohannis	38°53'44.98'' – 24°31'40.23''	Sky2a, Sky6	Magnetitite
	38°54'15.39'' – 24°32'38.05''	Sky3, Sky4 SK3A, SK3E, SK3H, SK3I	Serpentinitite Chromitite
Northern Agios Iohannis	38°54'10.68'' – 24°32'3.41''	SK4A, SK5	Chromitite - Serpentinitite
	38°53'30.22'' – 24°31'21.23''	Sky9, Sky10	Serpentinitite - Chromitite
Agia Alexandria	38°53'29.90'' – 24°31'27.12''	Sky11a, Sky13	Chromitite
		Sky14a, Sky14b SK13	Chromitite Magnetitite

Fig. 1 - (a) Major structural elements of the Aegean Sea region; modified after Zachariadis (2007); (b) Schematic geological map of the Skyros Island; modified after Papantoniou (2015). Yellow stars represent the three sampling locations. NAI: Northern Agios Iohannis; AI: Agios Iohannis; AA: Agia Alexandria.



MATERIALS AND METHODS

Altered peridotite, chromitite, and magnetite-rich samples were collected from small outcrops in the areas of Agios Iohannis, Northern Agios Iohannis, and Agia Alexandria (Table 1, Fig. 1b). Chromitites form small lenses (up to 1m in thickness) scattered into serpentinitized dunites (Fig. 2a). Chromitites are locally enriched in Cr-garnet, clearly visible at outcrop scale (Fig. 2b, c). Massive magnetites within serpentinitized peridotites also crop out in the area, forming pods (up to 60 cm thick) visually similar to chromitites (Fig. 2c), but highly magnetic. Most of the chromitite lenses were locally mined and stored in nearby heaps. Chromitites show disseminated, nodular, and massive textures (Fig. 2 d, e).

The samples were studied through optical microscopy in reflected and transmitted light. Mineral chemistry of major and accessory phases was analyzed through EMPA (Electron Microprobe Analyzer) at the Earth Science Department of the University of Milan (samples Sky8a, Sky8b, Sky10) and at the Eugen F. Stumpfl Laboratory at the University of Leoben (samples SK3A, SK3E, SK3H, SK3I) with a Jeol JXA 8200 electron microprobe equipped with a wavelength dispersive system (SEM-WDS). Analyzing conditions for oxides and silicates are: 15 kV, sample current 10 nA, counting time of 20s on the peaks and 10s on the background. The elements were analyzed using the $K\alpha$ line. A series of natural minerals was used as standards: wollastonite for Si, forsterite for Mg,

ilmenite for Ti, fayalite for Fe, anorthite for Al and Ca, chromite for Cr, niccolite for Ni, rhodonite for Mn and Zn, and metallic V for that element. The approximate detection limit is 0.01 wt% for each element. Fe^{3+} was recalculated from microprobe analyses assuming perfect stoichiometry, based on 8-oxygen formula. Base Metal Minerals and Platinum Group Minerals were analyzed with 20 kV accelerating voltage, 10 nA beam current, and beam diameter of about 1 micron. The peak and background counting times were 20 and 10s, respectively. The following lines were selected: $K\alpha$ for S, Ni, Fe and Cu, $M\alpha$ for Os and $L\alpha$ for As, Sb, Ir, Ru, Rh, Pd, and Pt. The standards employed were: chalcopyrite (Cu), pyrite (Fe,S), niccolite for As and Ni, pure metals for Ru, Rh, Pd, Os, Ir and Pt. Microprobe analyses of magnetite and garnet are sometimes above 100 wt% because of the stoichiometric recalculation of Fe^{3+} and Fe^{2+} . Serpentine and chlorite are below 100% on average due to possible non-stoichiometric water contents and their lamellar shape.

Whole-rock PGE analyses were performed on chromitites and magnetite samples from Skyros Ophiolite at the National Research Center of Geo-analysis, Chinese Academy of Sciences (CAS), through Inductively Coupled Plasma Mass Spectrometry (ICP-MS) after a pre-concentration stage with nickel sulfide fire-assay collection. The precision of the analysis is better than 5% for Rh, Pd, and Ir, and 10% for the other elements. The detection limits are 0.2 ppb for Pt and Pd, 0.001 ppb for Ir, Rh and Os, and 0.1 ppb for Ru.

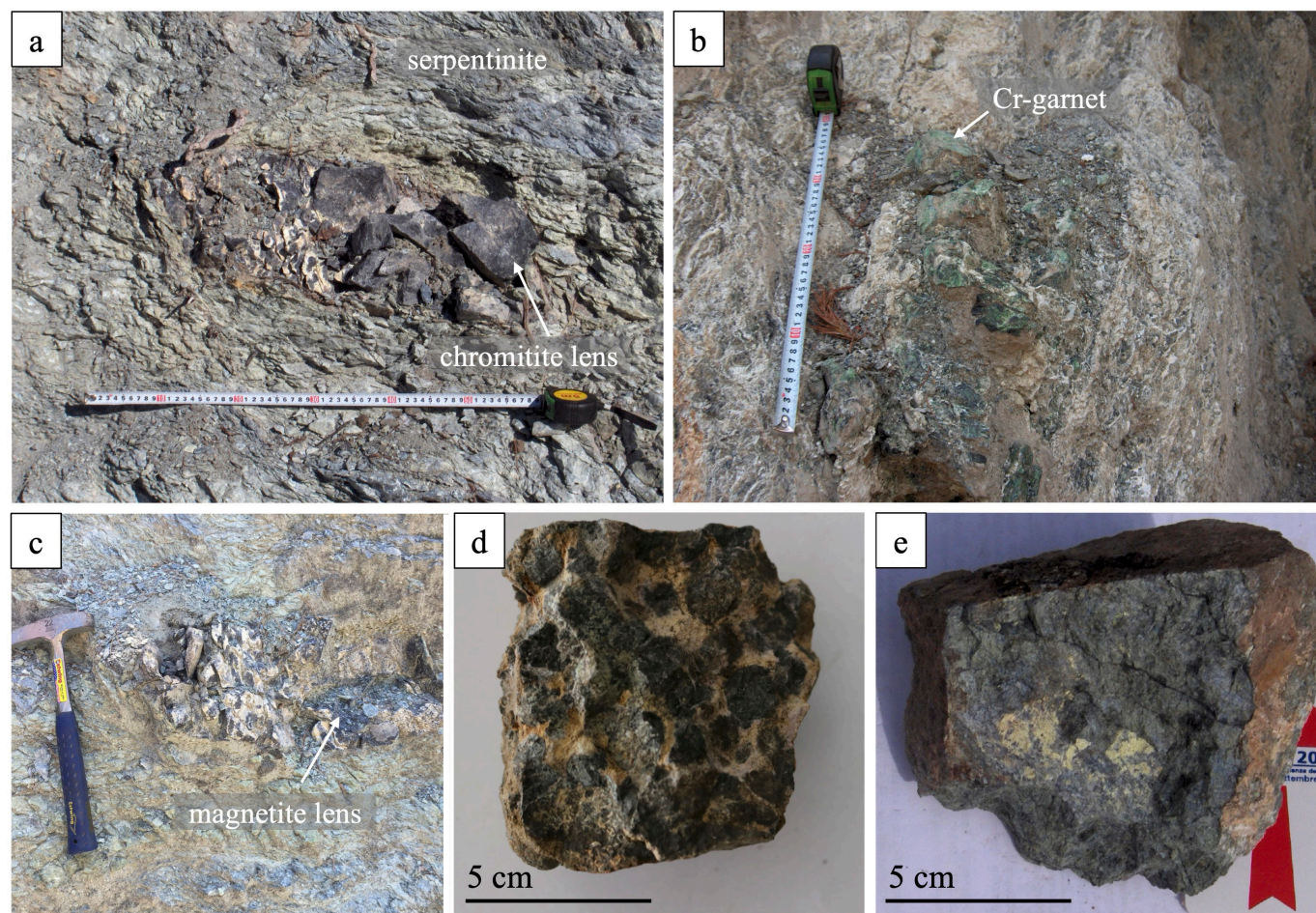


Fig. 2 - (a) Centimetric pod of massive chromitite in serpentinite from Agia Alexandria; (b) Garnet-bearing chromitite in serpentinite from Northern Agios Iohannis; (c) Magnetite pod within serpentinitized peridotite at Agios Iohannis; (d) Chromitite with nodular texture from Agios Iohannis; (e) Chromitite with massive texture from Northern Agios Iohannis.

RESULTS

Mineralogy and texture

Cr-spinels form anhedral to subhedral heavily fractured crystals (Fig. 3a), with widespread alteration into ferrian-chromite at the rims and along fractures (Fig. 3b). Primary silicates underwent alteration and are almost completely replaced by secondary phases (serpentine, chlorite), with only a few primary pyroxene relics detected in the samples from Agios Iohannis. A peculiar feature of Agios Iohannis and Northern Agios Iohannis chromitites is the presence of thick Cr-garnet coronas developed around chromite and occasionally filling the fractures (Fig. 3a, c). Base Metal Minerals and Platinum Group Minerals are present as rare accessory phases, and comprise heazlewoodite, millerite, pentlandite, Ni-arsenides, awaruite, Ni-Fe-Cu alloy, laurite, garutiite (Fig. 3d), and a Rh-rich sulfide.

Mineral and Whole Rock Chemistry

Average composition and standard deviations of spinels, silicates, and base metal minerals are reported in Tables 2, 3, and 4. Complete analyses are reported in the Supplementary material.

Spinel Mineral Chemistry

Skyros chromitites are characterized by spinels with variable compositions, concerning in particular major elements of unaltered chromites (Table 2).

Unaltered chromite from Agios Iohannis has Cr_2O_3 , Al_2O_3 , and Fe_2O_3 contents ranging between 52.98-54.57 wt%, 16.18-17.92 wt%, and 1.71-2.99 wt% respectively. FeO and MgO vary between 11.81-14.15% and 14.12-15.00 wt%. Alteration in ferrian-chromite is marked by a decrease in Al_2O_3 (0.70-2.47), a slight increase in Cr_2O_3 (47.58-56.89 wt%), and an increase in Fe_2O_3 (8.56-18.46 wt%). FeO and MgO are also affected by ferrian-chromitization and vary

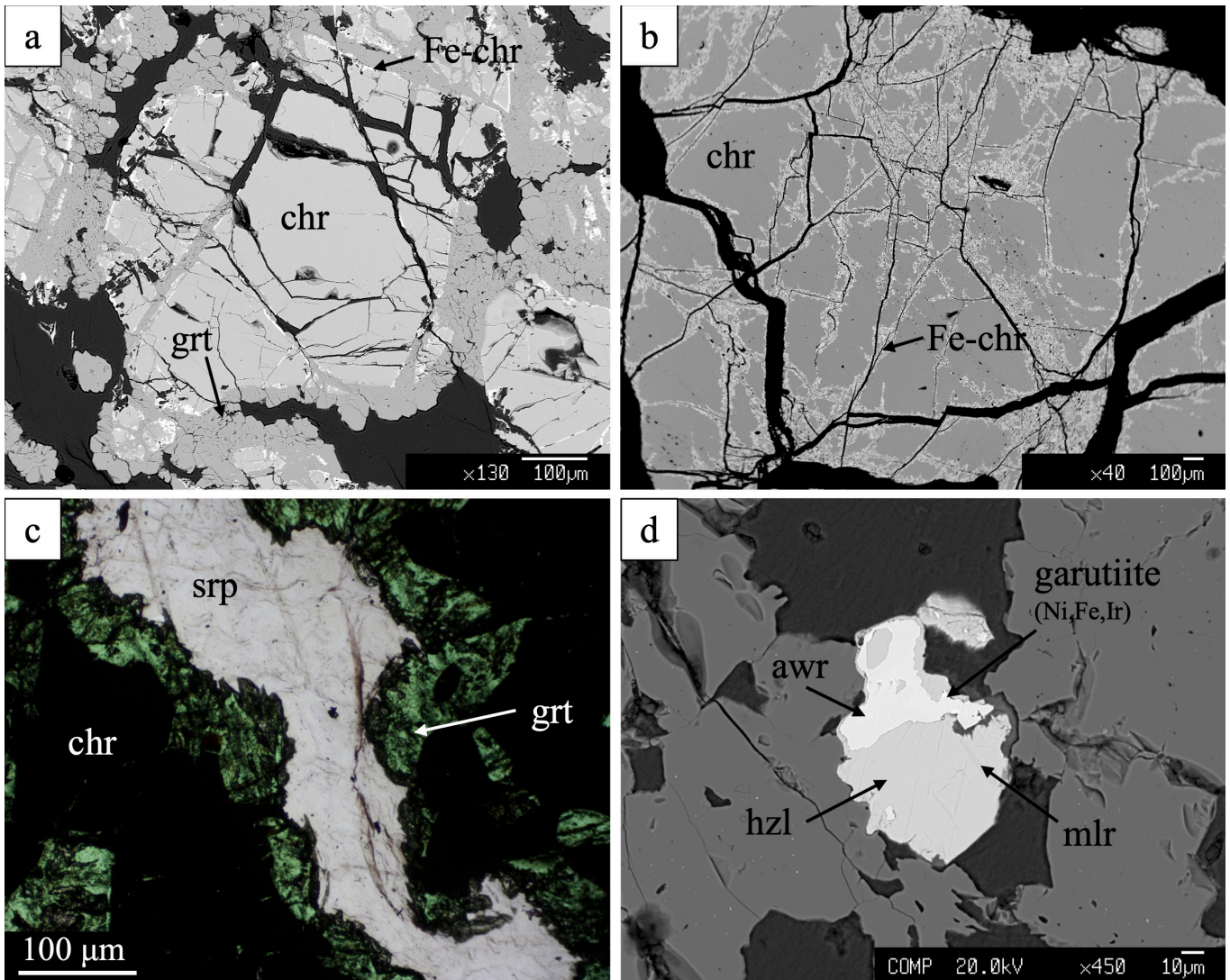


Fig. 3 - (a) BSE image of fractured chromite crystal surrounded by Cr-garnet coronae at Agios Iohannis; (b) BSE image of ferrian chromite alteration along cracks and chromite rims at Agia Alexandria; (c) transmitted light microphotograph of Cr-garnet coronae in contact with serpentinic matrix and chromite crystals, at Northern Agios Iohannis; (d) BSE image of a heazlewoodite crystal with millerite exsolution lamellae, partially replaced by awaruite and associated to garutiite, at Northern Agios Iohannis. Mineral Abbreviations: chr: chromite; Fe-chr: ferrian-chromite; grt: garnet; srp: serpentine; awr: awaruite; hwl: heazlewoodite; mlr: millerite.

Table 2 - Average composition (wt%) and standard deviation of spinels from Agios Iohannis, Northern Agios Iohannis and Agia Alexandria.

	AGIOS IOHANNIS										NORTHERN AGIOS IOHANNIS										AGIA ALEXANDRIA				
	chromite avg (n=22)	st.dev.	Fe-chromite avg (n=11)	st.dev.	Cr-magnetite avg (n=7)	st.dev.	chromite avg (n=110)	stdev	Fe-chromite SK3A*	Cr-magnetite avg (n=3)	st.dev.	Cr-magnetite avg (n=10)	st.dev.	chromite avg (n=9)	st.dev.	Fe-chromite avg (n=14)	st.dev.	magnetite avg (n=5)	st.dev.						
SiO ₂	bdl	-	0.21	0.23	0.27	0.49	bdl	-	1.04	0.64	0.77	0.03	0.02	bdl	-	1.77	1.99	0.27	0.26						
TiO ₂	0.21	0.03	0.22	0.03	0.03	0.03	0.24	0.03	0.24	0.00	0.00	0.01	0.01	0.24	0.05	0.30	0.05	bdl	-						
Al ₂ O ₃	17.17	0.46	1.70	0.48	0.24	0.23	13.20	1.50	4.95	0.00	0.00	0.00	0.00	19.23	0.61	5.05	2.51	bdl	-						
Cr ₂ O ₃	53.86	0.40	52.57	3.26	16.39	13.28	54.93	2.35	52.87	4.82	2.84	0.22	0.21	52.10	0.40	60.36	4.39	bdl	-						
Fe ₂ O ₃	2.27	0.34	13.23	3.23	52.70	16.05	0.69	0.79	8.84	66.00	5.42	72.18	0.58	2.73	0.46	1.53	1.66	68.94	0.34						
FeO	12.84	0.65	17.64	3.34	29.23	3.25	16.97	1.72	20.77	30.30	1.88	32.20	0.19	12.47	0.40	20.75	2.77	30.86	0.33						
MnO	bdl	-	9.51	2.06	2.32	2.52	bdl	-	1.70	0.53	0.24	0.18	0.05	bdl	-	0.43	0.15	0.28	0.05						
MgO	14.65	0.24	3.16	0.89	0.43	0.28	10.56	0.94	7.22	1.47	1.24	0.12	0.01	15.35	0.31	8.97	2.80	0.32	0.11						
total	101.09	1.00	98.23	1.03	101.61	2.81	96.78	0.86	97.61	103.77	2.15	104.95	0.70	102.22	0.47	99.16	2.36	100.71	0.36						
Si	0.001	0.001	0.008	0.009	0.010	0.019	0.003	0.010	0.037	0.024	0.028	0.001	0.001	0.001	0.001	0.059	0.065	0.010	0.010						
Ti	0.005	0.001	0.006	0.001	0.001	0.001	0.006	0.001	0.006	0.000	0.000	0.000	0.000	0.005	0.001	0.008	0.001	0.000	0.000						
Al	0.623	0.012	0.074	0.020	0.011	0.010	0.520	0.057	0.206	0.000	0.000	0.000	0.000	0.683	0.017	0.200	0.093	0.001	0.000						
Cr	1.312	0.016	1.531	0.085	0.490	0.401	1.451	0.064	1.474	0.140	0.083	0.006	0.006	1.242	0.016	1.633	0.151	0.000	0.001						
Fe ³⁺	0.053	0.008	0.367	0.092	1.477	0.430	0.017	0.020	0.235	1.813	0.137	1.991	0.006	0.062	0.010	0.040	0.046	1.977	0.020						
Fe ²⁺	0.331	0.014	0.544	0.103	0.913	0.088	0.474	0.048	0.612	0.925	0.052	0.987	0.003	0.314	0.011	0.595	0.100	0.984	0.006						
Mn	0.002	0.001	0.297	0.065	0.074	0.081	0.003	0.003	0.051	0.016	0.007	0.006	0.002	0.002	0.001	0.013	0.005	0.009	0.002						
Mg	0.673	0.015	0.173	0.049	0.024	0.016	0.526	0.047	0.380	0.081	0.068	0.007	0.001	0.690	0.010	0.452	0.125	0.018	0.006						
Mg#	0.670	0.014	0.246	0.079	0.027	0.019	0.526	0.047	0.383	0.079	0.066	0.007	0.001	0.687	0.011	0.429	0.105	0.018	0.006						
Cr#	0.678	0.007	0.954	0.011	0.983	0.010	0.736	0.030	0.878	1.000	0.000	0.988	0.008	0.645	0.008	0.890	0.052	0.130	0.291						
Cr*#	0.660	0.008	0.776	0.040	0.249	0.206	0.730	0.031	0.770	0.072	0.044	0.003	0.003	0.625	0.008	0.871	0.046	0.000	0.000						

Fe₂O₃ and FeO are recalculated according to stoichiometry.

Table 3 - Average composition (wt%) and standard deviation of the silicate assemblage in Agios Iohannis, Northern Agios Iohannis and Agia Alexandria.

	AGIOS IOHANNIS												NORTHERN AGIOS IOHANNIS												AGIA ALEXANDRA	
	enstatite			diopside			serpentine			chlorite			garnet			serpentine			chlorite			garnet			chlorite	
	avg (n=4)	st.dev.		avg (n=3)	st.dev.		avg (n=8)	st.dev.		avg (n=12)	st.dev.		avg (n=10)	st.dev.		avg (n=13)	st.dev.		avg (n=16)	st.dev.		avg (n=122)	st.dev.	avg (n=8)	st.dev.	
SiO ₂	58.84	0.21		54.94	0.52		42.80	0.45		32.95	1.18		36.43	0.86		39.94	1.69		34.75	1.79		34.47	1.08		29.73	0.83
TiO ₂	0.05	0.03		0.11	0.03		0.02	0.03		0.01	0.01		0.08	0.04		0.01	0.02		0.04	0.02		0.08	0.05		0.01	0.01
Al ₂ O ₃	0.58	0.06		1.07	0.22		0.79	0.13		14.51	0.72		0.20	0.04		0.98	0.97		9.12	3.04		0.13	0.18		17.04	1.66
Cr ₂ O ₃	0.76	0.17		1.56	0.17		bdl	-		2.22	1.98		12.08	1.10		bdl	-		2.70	1.59		13.06	1.92		4.14	1.08
Fe ₂ O ₃	bdl	-		bdl	-		bdl	-		bdl	-		20.05	3.44		bdl	-		bdl	-		21.41	2.08		bdl	
FeO	3.45	0.20		1.63	0.13		2.27	0.46		0.62	0.16		1.75	1.16		2.01	0.34		1.26	0.54		0.89	1.02		0.63	0.15
MnO	0.08	0.01		0.07	0.05		0.06	0.02		0.03	0.02		0.01	0.01		0.02	0.02		0.02	0.02		0.04	0.04		0.00	0.00
MgO	36.25	0.44		17.90	0.18		38.69	0.61		34.09	0.74		0.08	0.07		37.90	1.86		35.48	1.41		0.32	1.45		33.64	0.65
CaO	0.49	0.07		23.04	0.31		0.08	0.04		0.01	0.01		32.58	0.17		0.07	0.03		0.03	0.02		30.99	1.24		0.02	0.01
Na ₂ O	0.01	0.01		0.34	0.02		0.01	0.01		0.01	0.01		-	-		0.01	0.01		0.01	0.01		-	-		0.01	0.02
H ₂ O*	-	-		-	-		12.41	0.06		12.13	0.27		-	-		11.98	0.32		11.97	0.20		-	-		12.02	0.19
total	100.49	0.51		100.66	0.83		98.01	0.65		96.59	0.52		103.26	1.35		93.76	2.65		95.37	1.39		101.28	1.42		97.22	0.94
Si	2.000	0.011		1.980	0.003		4.083	0.022		3.226	0.054		2.979	0.083		3.997	0.152		3.482	0.164		2.882	0.065		2.967	0.071
Ti	0.001	0.001		0.003	0.001		0.002	0.002		0.001	0.001		0.005	0.002		0.001	0.001		0.003	0.002		0.005	0.003		0.000	0.001
Al	0.023	0.002		0.045	0.009		0.089	0.015		1.675	0.082		0.019	0.004		0.114	0.111		1.077	0.359		0.013	0.018		2.003	0.181
Cr	0.020	0.004		0.044	0.005		0.000	0.000		0.265	0.237		0.781	0.073		0.000	0.000		0.322	0.192		0.864	0.134		0.491	0.131
Fe ₃	0.000	0.000		0.000	0.000		0.000	0.000		0.000	0.000		1.232	0.205		0.000	0.000		0.000	0.000		1.347	0.131		0.000	0.000
Fe ₂	0.098	0.006		0.049	0.004		0.181	0.038		0.051	0.013		0.120	0.080		0.168	0.029		0.106	0.045		0.061	0.070		0.053	0.013
Mn	0.002	0.000		0.002	0.002		0.005	0.001		0.002	0.002		0.001	0.001		0.002	0.002		0.001	0.002		0.002	0.003		0.000	0.000
Mg	1.837	0.011		0.962	0.002		5.502	0.066		4.978	0.056		0.010	0.009		5.654	0.257		5.302	0.207		0.040	0.184		5.006	0.151
Ca	0.018	0.003		0.890	0.013		0.008	0.004		0.001	0.001		2.854	0.027		0.007	0.003		0.003	0.002		2.777	0.111		0.002	0.001
Na	0.000	0.001		0.024	0.001		0.002	0.002		0.002	0.003		0.001	0.001		0.001	0.002		0.002	0.003		0.003	0.002		0.002	0.004
OH*				8.000	0.000		8.000	0.000		8.000	0.000		8.000	0.000		8.000	0.000		8.000	0.000		8.000	0.000		8.000	0.000

H₂O and OH recalculated according to stoichiometry.

between 11.93-26.44 wt% and 1.59-4.94 wt%. An interesting feature of Fe-chromites in Agios Iohannis is a high Mn content (MnO 3.99-12.01 wt%). The following alteration stage involves the formation of Cr-magnetite, leading to a complete loss of Al₂O₃, a decrease in Cr₂O₃ (3.20-32.82 wt%), and further increase in Fe₂O₃ (33.60-68.41 wt%). FeO and MgO vary between 24.79-32.23 wt% and 0.14-0.77 wt%.

Unaltered chromite from Northern Agios Iohannis has Cr₂O₃, Al₂O₃, and Fe₂O₃ contents ranging between 42.69-58.03 wt%, 11.37-19.00 wt% and up to 3.00 wt% respectively. FeO and MgO vary between 14.51-24.41 wt% and 6.81-12.07 wt%. Fe-chromitization is marked by a decrease in Al₂O₃ (4.95 wt%) and increase in Fe₂O₃ (8.84 wt%). Cr-magnetite shows lower Cr₂O₃ contents (1.77-7.45 wt%) and higher Fe₂O₃ contents (60.42-69.21 wt%). FeO varies between 28.97-31.52 wt% and MgO contents are between 0.12-2.55 wt%. Magnetite Al₂O₃, Cr₂O₃ and MgO contents are below detection limit. Fe₂O₃ and FeO contents vary between 70.66-72.36 wt% and 31.50-32.17 wt%.

Unaltered chromite from Agia Alexandria is more similar to Agios Iohannis, with Cr₂O₃, Al₂O₃, and Fe₂O₃ contents ranging between 51.39-52.75 wt%, 18.19-20.07 wt% and 2.18-3.51 wt%. FeO and MgO vary between 11.87-13.03 wt% and 14.74-15.81 wt%. Alteration into ferrian-chromite is marked by a decrease in Al₂O₃ (1.89-9.16 wt%) and MgO (4.77-14.18 wt%) and by an increase in Cr₂O₃ (48.45-65.12 wt%), Fe₂O₃ (up to 5.85 wt%) and FeO (16.99 - 25.70 wt%). Notably, the enrichment in Mn is absent in Agia Alexandria. Magnetite has Fe₂O₃ contents ranging between 68.55 and 69.38 wt%, and FeO contents ranging between 30.52 and 31.26 wt%.

Silicate Mineral Chemistry

Primary silicate relicts from Agios Iohannis are enstatite and diopside crystals. Orthopyroxene has MgO and FeO contents of 3.19-3.66 wt% and 35.84-36.85 wt%. Cr₂O₃ and Al₂O₃ vary between 0.51-0.91 and 0.52-0.65 wt% respectively. Clinopyroxene has MgO and CaO contents of 17.77-18.10 wt% and 22.71-23.33 wt%, and higher Cr₂O₃ and Al₂O₃ contents, varying between 1.38 and 1.72 wt% and 0.91-1.32 wt% respectively.

Serpentine is present in Agios Iohannis and Northern Agios Iohannis as the major silicate alteration phase. In Agios Iohannis MgO and FeO contents range between 37.27-39.21 wt% and 1.68-3.18 wt%, while in Northern Agios Iohannis MgO and FeO contents range between 38.25-40.16 and 1.59-2.69 wt%.

Chlorite was detected in all three localities, with vari-

able Cr₂O₃ contents. In Agios Iohannis FeO, MgO and Cr₂O₃ range between 0.37-0.89 wt%, 33.05-35.18 wt% and bdl-4.94 wt%. Chlorite from Northern Agios Iohannis has higher FeO (0.72-2.34 wt%), MgO comprised between 33.03 and 38.28 wt% and Cr₂O₃ ranging from 0.24 to 4.63 wt%. Agia Alexandria shows low FeO contents (0.43-0.90 wt%), MgO between 33.21 and 35.19 wt% and Cr₂O₃ between 2.20 and 5.04 wt%.

Garnets were detected in Agios Iohannis and Northern Agios Iohannis. They are all solid solutions between andradite and uvarovite (Fig. 5b), with variable iron and chromium contents. Northern Agios Iohannis garnets have highly variable Cr₂O₃ (8.82-20.83 wt%), Fe₂O₃ (14.57-33.04 wt%), FeO (bdl-3.52 wt%), MgO (bdl-13.65 wt%) and CaO (20.65-32.09 wt%) contents. In Agios Iohannis Cr₂O₃ contents range between 9.40-12.95 wt%, Fe₂O₃ contents between 12.06-24.72 wt%, FeO contents

Base Metal and PGM Mineral Chemistry

Base Metal Minerals within Skyros samples are mainly Ni-Fe phases, with rare Cu-bearing sulfides and Ni-arsenides. Platinum Group Minerals are rare and mostly too tiny for microprobe analysis. Pentlandite, detected in Agios Iohannis and Northern Agios Iohannis, shows little variability, with Ni (37.71-43.18 wt%) and Fe (22.44-24.26 wt%). Millerite and heazlewoodite were detected in all three localities. Millerite Ni content varies between 63.39 and 72.60 wt%, and the iron content varies from below detection limit up to 1.52 wt%. Heazlewoodite also shows a moderate variability in Ni content, from 61.05 to 76.95 wt%, and the Fe content varies from below detection limit up to 3.27 wt%. Ni-Fe alloys have been detected only in Agios Iohannis and Northern Agios Iohannis and they consist mostly of awaruite (Ni 73.98-83.12 wt%, Fe 5.25-23.18 wt%) and one Fe-Ni alloy with Fe content of 63.12 wt%.

Rare Platinum Group Minerals were detected in Northern Agios Iohannis, but the alteration and grain size did not allow a proper quantification. From EDS data the PGM detected are a tiny garutiite crystal, a laurite and a Rh-rich sulfide (see Supplementary Material).

PGE whole rock chemistry

The total PGE content (Table 5) of Skyros chromitites ranges between 72 and 246 ppb, while the two analyzed magnetitites show enrichments of 17 ppb (Agia Alexandria) and 174 ppb (Agios Iohannis). Northern Agios Iohannis is the locality with the highest PGE total content, in agreement with the few Platinum Group Minerals detected in the same locality.

Table 5 - PGE whole rock chemistry (ppb) of Skyros chromitites and magnetite.

Sample	Lithology	Os	Ir	Ru	Rh	Pt	Pd	Total PGE
Sky-8a	AI - chromitite	33	25	54	4	2	2	120
Sky-8b	AI - chromitite	5	12	45	6	3	1	72
Sky-6	AI - magnetite	11	28	56	10	40	29	174
Sky-10	AA - chromitite	15	16	52	7	1	2	93
Sky-11a	AA - chromitite	28	19	67	6	1	2	123
SK-13	AA - magnetite	1	2	4	5	3	2	17
SK-4a	NAI - chromitite	69	49	98	10	16	4.03	246

DISCUSSION

Skyros tectonic setting and magmatic evolution

The composition of Skyros unaltered chromite is variable among the different localities (Fig. 4a). Chromites from Agios Iohannis and Agia Alexandria show high Mg# and relatively low Cr#, Agios Iohannis and are consistent with published data on Skyros chromitites (Economou-Eliopoulos, 1996). Northern Agios Iohannis chromites, on the other hand, have higher Cr#, more similar to Gerakini and Vavdos chromitites, located in the Vardar Domain in the Chalkidiki Peninsula.

High-Cr chromitites are generally thought to indicate a genesis from high degrees of partial melting, from boninitic melts (Barnes and Roeder, 2001). Chromites from Agios Iohannis and Agia Alexandria have a forearc geodynamic affinity (Fig. 4b), while chromites from Northern Agios Iohannis show an increase in Cr# towards a boninitic affinity. Bimodal chromite mineral chemistry in supra-subduction settings is commonly attributed to an evolution from MORB-like to IAT and boninitic melts at different times during the evolution of the subduction zone, and has been reported also within ophiolites of the Albanide-Hellenide belt (Bussolesi et al., 2022a; Qiu et al., 2018; Saccani et al., 2017; Saccani and Tassinari, 2015; Uysal et al., 2009; Xiong et al., 2017).

The genetical models of chromitites must also be considered. Chromite ore bodies in supra-subduction settings form within restitic “dunite channels”, where the ascending melts

percolate and mix (Cocomazzi et al., 2020; Spiegelman and Kelemen, 2003). When magmas with different composition mix, chromite precipitation can be triggered, and chromite mineral chemistry will partially depend on the chemistry of the magma. Another possible explanation for the heterogeneity of spinel mineral chemistry can be derived from the theory that podiform chromitites are the product of melt/rock interaction. Melts interacting with variably depleted peridotite sources will produce high-Al or high-Cr chromitites (Zhou et al., 2001). Considering the geographic proximity of Skyros chromite bodies, they may be indeed have formed in different dunite channels by the mixing of magmas with different composition (Ballhaus, 1998; Miura et al., 2012). Finally, considering the nature of the subophiolitic mélange (Bortolotti and Principi, 2005), it is also possible that the outcrops, now geographically close, belong to different tectonic slices of mantle with variable composition, later dismembered and tectonically juxtaposed during obduction.

Skyros post-magmatic evolution

Skyros chromitites and host rocks are heavily altered, as testified by widespread replacement of primary silicates by serpentine and chlorite (Fig. 3c). Various alteration stages affected also chromite crystals, partially replaced by ferri-chromite and Cr-magnetite (Fig. 5a) at the rims, and surrounded by Cr-garnets coronas, formed at the expense of spinel and serpentine (Frost and Beard, 2007).

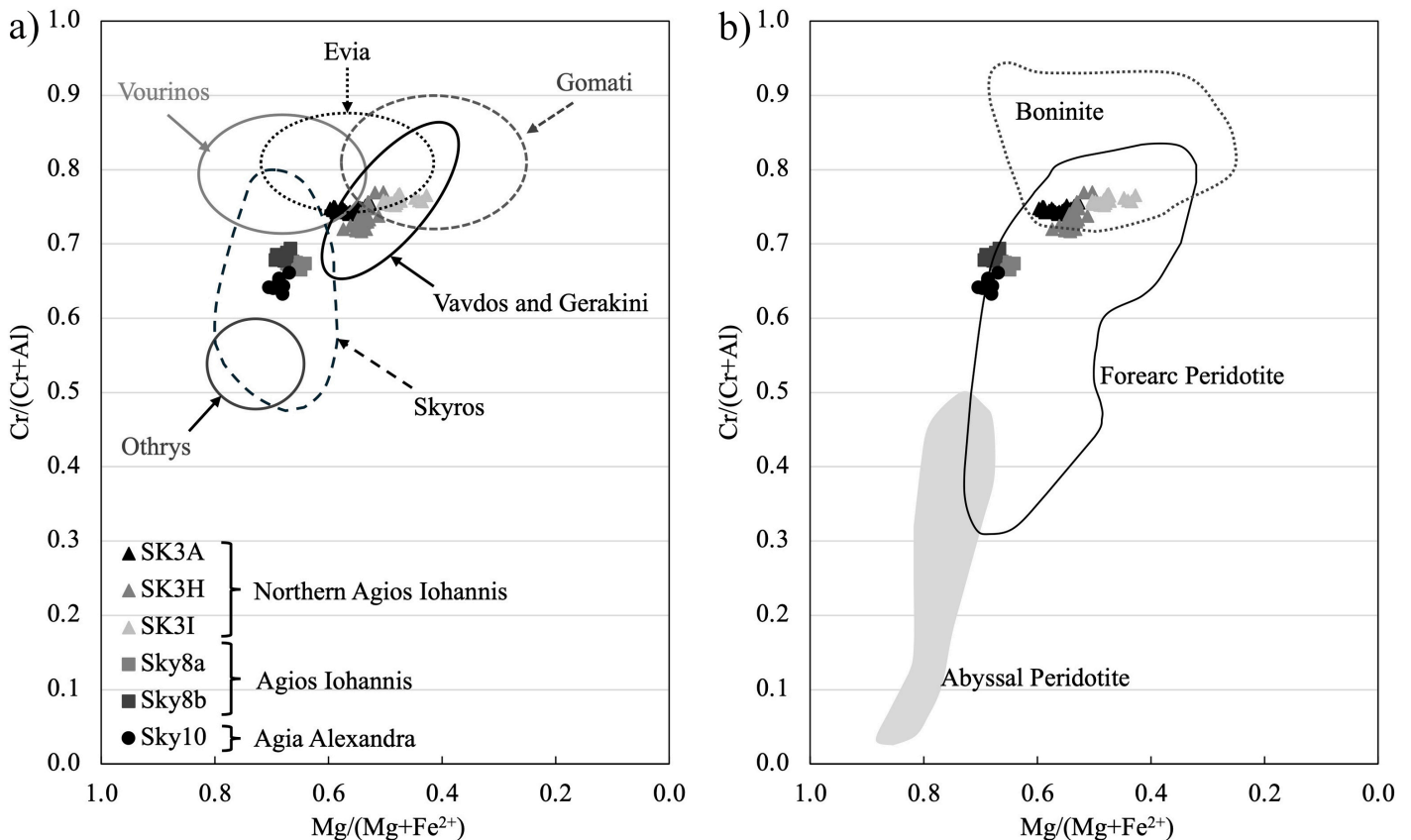


Fig. 4 - (a) Mg# vs Cr# of Skyros unaltered spinels; compositional fields of Vourinos (Grieco et al., 2018), Vavdos (Grieco et al., 2011; Sideridis et al., 2021), Skyros (Economou-Eliopoulos, 1996), Othrys (Kapsiotis et al., 2018), Evia (Grieco et al., 2023) and Gomati (Bussolesi et al., 2020; 2022b) are used for comparison; (b) fields for abyssal peridotite, forearc peridotite and boninite are from Barnes and Roeder (2001).

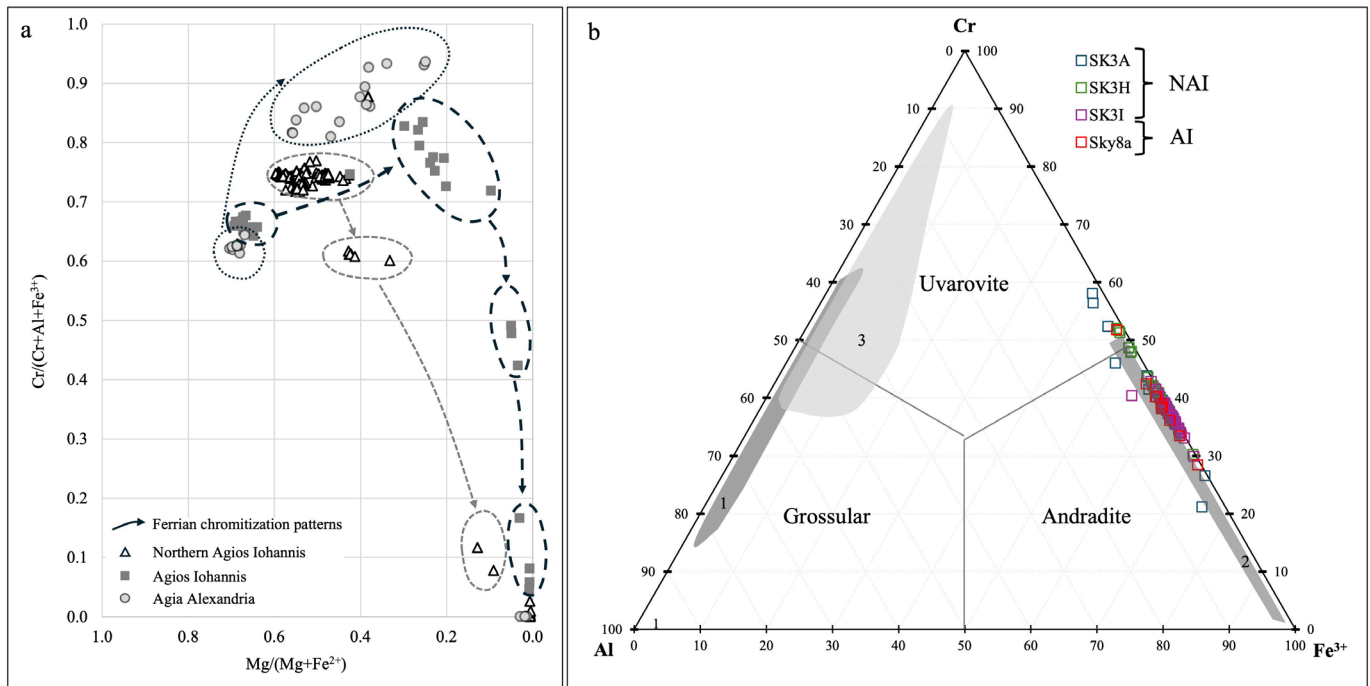
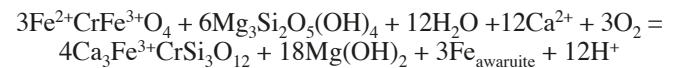


Fig. 5 - (a) ferrian chromitization patterns; (b) Cr-garnet composition (mol%) compared to 1. Cr-garnets from Moa Baracoa podiform chromitites (Proenza et al., 1999), 2. Cr-garnets from Rutland podiform chromitites (Ghosh and Morishita, 2011) and 3. Cr-garnets from the Chalkidiki peninsula (Sideridis et al., 2022).

The first alteration stage detected at Skyros was serpentinization. As Skyros peridotites are largely represented by harzburgites and dunites (Karkalis et al., 2017), the most common serpentinization reaction must have been the transformation of olivine into serpentine, even though no relicts of olivine have been detected. Enstatite and diopside were also engaged in the serpentinization reaction, the latter one involving also the release of Ca^{2+} in the hydrothermal fluids (Frost and Beard, 2007). The second alteration event involves the circulation of fluids and the formation of ferrian-chromite and chromian-chlorite at the expense of chromite and serpentine (Merlini et al., 2009). At Northern Agios Iohannis and Agios Iohannis the alteration is more pronounced: extreme ferrian-chromitization led to transformation of the spinel into Cr-magnetite, while at Agia Alexandria spinels are less altered (Fig. 5a). The enrichment in Mn within Fe-chromite and magnetite at Agios Iohannis and Northern Agios Iohannis can also be attributed to alteration or metasomatic processes during this stage (Paraskevopoulos and Economou (1981) reported similar Mn-rich ferrian-chromites within serpentinites in Northern Greece, where Mn is highly enriched in ferrian-chromites and decreases again in Cr-magnetite rims. This enrichment is attributed to Mn substituting Mg and Fe^{2+} , where Mn derives from chromite already transformed into Cr-magnetite or magnetite.

The third alteration event led to precipitation of garnet as coronas surrounding chromite grains. The detected garnets show a wide range of compositions along the andradite-uvarovite solid solution (Fig. 5b). Uvarovitic garnets have been detected in chromitite deposits, with solid solutions ranging between uvarovite-andradite and uvarovite-grossular (Chakraborty, 1968; Ghosh and Morishita, 2011; Frank Melcher et al., 1997; Proenza et al., 1999; Sideridis et al., 2022). Their genesis is interpreted as the result of the circulation of a hydrothermal fluid through the chromitites and their

hosts. The source of Ca^{2+} is under debate. The breakup of clinopyroxene during serpentinization is one of the possible local sources of Ca^{2+} (Ghosh and Morishita, 2011; Pal and Das, 2010), but Skyros chromitites are surrounded by Ca-bearing rocks (ophicalcites, calcite blue-schists and marbles), that could provide another Ca source for the formation of the garnets. The Cr-Fe instead of Cr-Al substitution in the garnet solid solution is possibly explained by the reaction of Al-poor ferrian-chromite with hydrothermal fluids and serpentine to form the garnet coronas replacing the spinel (Fig. 6). (Frost and Beard (2007) propose a reaction for the formation of andradite from magnetite and serpentine. The reaction is here modified to accommodate Cr, so that Cr-garnet is formed by the reaction of Fe-chromite and serpentine in the presence of aqueous fluids:



Following this interpretation, the source of Ca^{2+} is most likely external, from Ca-bearing host rocks, since Ca^{2+} was liberated during clinopyroxene alteration into serpentine in the first alteration stage, whereas garnets were formed later on.

One of the most distinctive features of serpentinized rocks is the extremely low oxygen fugacity, as indicated by the presence of Ni-Fe alloys (Frost, 1985). The occurrence of Ni-Fe alloys instead of sulfides suggests that serpentinization occurs at low $f\text{S}_2$ as well as low $f\text{O}_2$. The replacement of primary silicates by serpentine releases some H_2 (Bach et al., 2006), which can combine with $\frac{1}{2}\text{O}_2$ to form H_2O and/or with S to form H_2S , lowering $f\text{O}_2$ and $f\text{S}_2$. As oxygen fugacity falls, sulfides become poor in sulfur, forming millerite, heazlewoodite, and metal alloys (Frost and Beard, 2007).

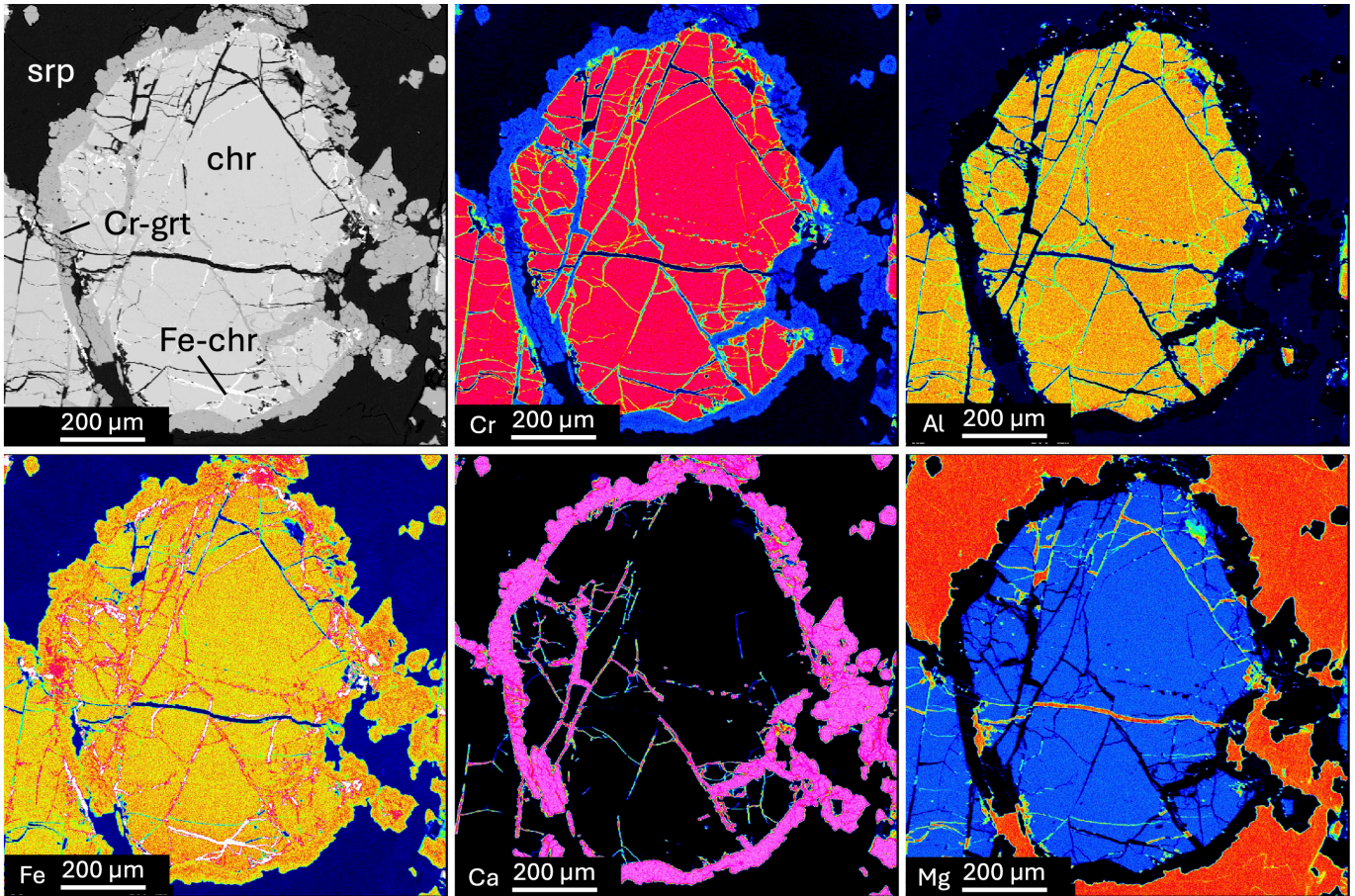


Fig. 6 - X-ray elemental maps of chromite surrounded by Cr-garnet corona at Agios Iohannis locality; grt, garnet; chr, chromite.

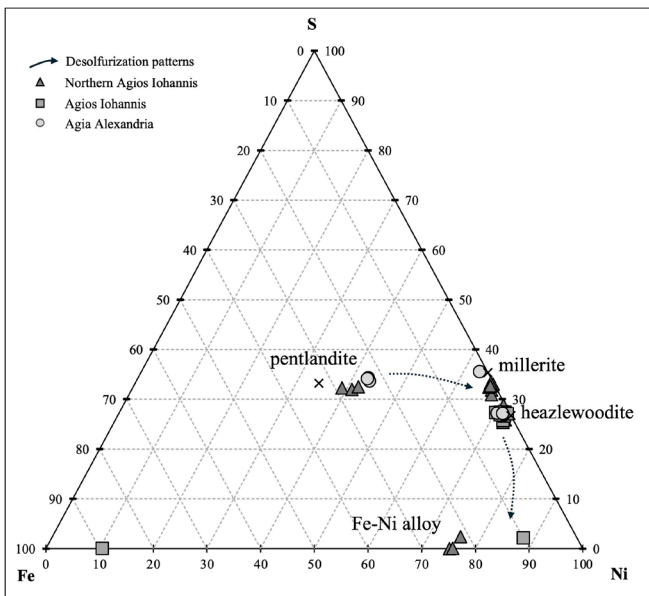


Fig. 7 - Fe-Ni-S compositional diagram of Base Metal Minerals within Skyros chromitites.

Agios Iohannis and Northern Agios Iohannis show a desulfurization pattern typical of serpentinization (Fig. 7), with primary pentlandites changed into Ni-Fe alloys during the first alteration stage. On the contrary, Agia Alexandria

mineral assemblage lacks alloys, suggesting a more limited first alteration stage, whereas the abundance of chlorite may indicate a fluctuation of fO_2 towards higher values during the second alteration event. The third alteration event, related to garnet formation, is absent in Agia Alexandria either for lack of circulation of fluids or because the garnet-forming reaction was not triggered in the presence of widespread chlorite.

PGE contents in Skyros chromitites are consistent with PGE-poor podiform chromitites worldwide, with the richest sample being Northern Agios Iohannis, but the total PGE values are considerably lower than existing bibliographic data on Skyros chromitites (Tarkian et al., 1992; Economou-Eliopoulos, 1996), implying a high magmatic heterogeneity in the PGE budget of the parental melt. Chromitite mantle-normalized patterns (Fig. 8a) show a general negative slope from IPGE to PPGE, a very common trait of podiform chromitites worldwide explained by the different geochemical behavior of PGE in the mantle (Economou-Eliopoulos, 1996; Proenza et al., 2007; Uysal et al., 2009; Grieco et al., 2020; Bussolesi et al., 2022b). An interesting feature is the double-peak for Os and Ru, which is interpreted in the literature as a clue of PGE remobilization during serpentinization events, related in particular to desulfurization (Grieco et al., 2020).

Magnetite mantle-normalized patterns (Fig. 8b) are different for the two localities. Agia Alexandria is PGE-poor compared to mantle values, except for Rh, which is unusually enriched (5 ppb) and forms a positive anomaly. Agios Iohannis magnetitite has total PGE values comparable to

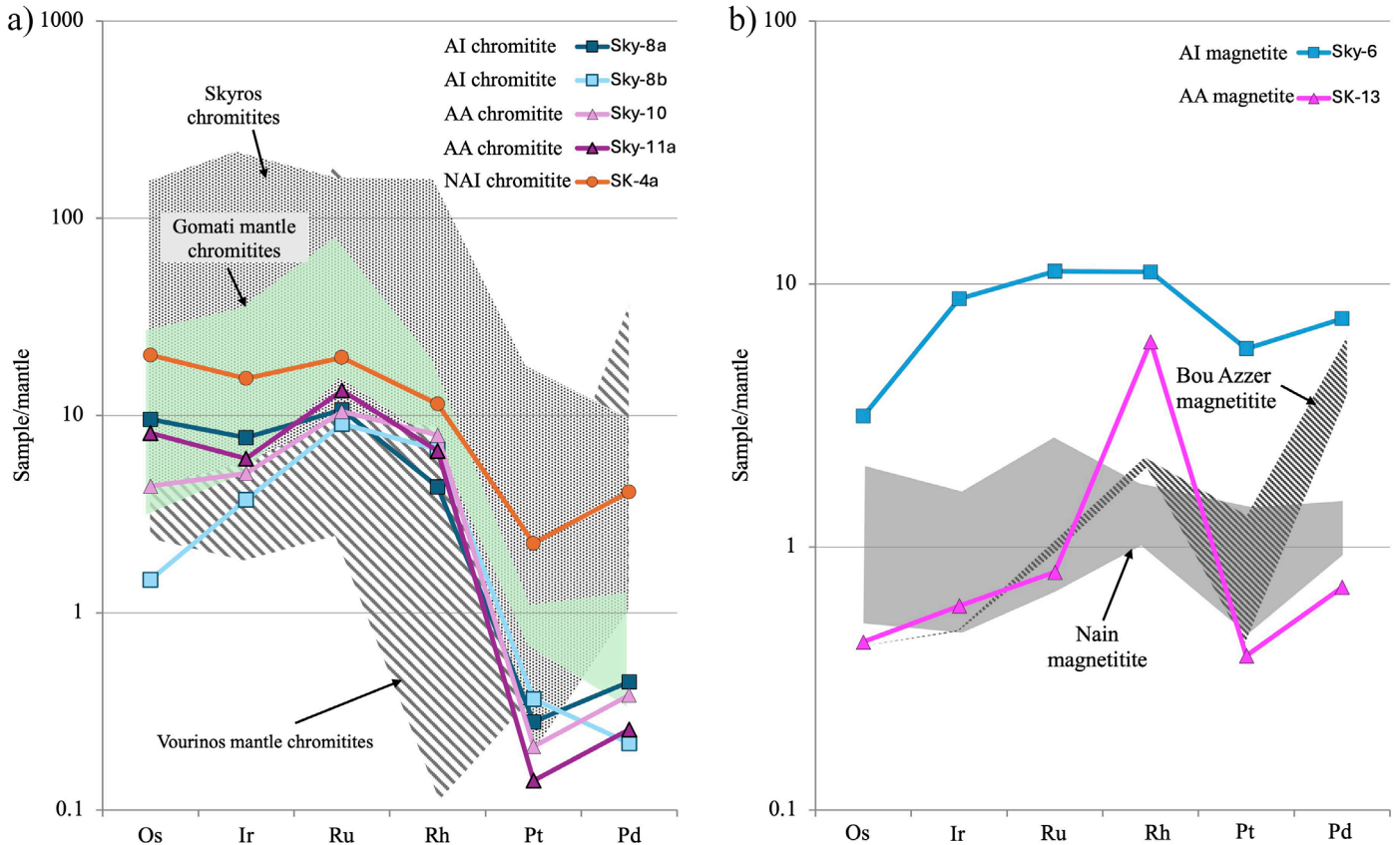


Fig. 8 - a) Mantle-normalized (McDonough and Sun, 1995) PGE patterns of Skyros chromitites; data for Gomati mantle chromitites from Bussolesi et al. (2022b); data for Vourinos chromitites from Grammatikopoulos et al. (2011); data for Skyros chromitites from Economou-Eliopoulos (1996) and Tarkian et al. (1992); b) Mantle normalized PGE patterns of Skyros magnetites; data for Nain magnetite from Eslami et al. (2018); data for Bou Azzer magnetite from Ahmed et al. (2009). AI: Agios Iohannis, AA: Agia Alexandria, NAI: Northern Agios Iohannis.

chromitites, with a slight enrichment in PPGE. PGE-poor Agia Alexandria magnetite patterns are comparable to other ophiolite magnetite deposits, indicating a low-T genesis as replacing products of mantle peridotites (dunite or harzburgite) through circulation of serpentinizing fluids (Ahmed et al., 2009; Eslami et al., 2018). This indicates a high Fe mobility from the protolith (dunite or harzburgite) into the newly formed magnetite ore. PGE patterns are indeed consistent with mantle serpentinized patterns, and the positive Rh anomaly could be due to a more immobile behavior of Rh during alteration events. Agios Iohannis enrichment in PGE, similar to ophiolitic chromitites patterns, suggests that the protolith of this magnetite nodule may have been a chromite instead of a harzburgite/dunite (that never reach PGE contents comparable to chromitites), where Cr-spinels were completely altered into magnetite during serpentinization.

CONCLUSIONS

Skyros podiform chromitites, albeit in a restricted geographical area, are heterogeneous from the mineralogical and chemical point of view. Chromites from Northern Agios Iohannis have a higher Cr content with respect to Agios Iohannis and Agia Alexandria, reflecting either a parent melt composition more evolved towards a boninitic affinity and/or a difference in the chemical composition of the parental magma. Post magmatic processes affected the three localities at different degrees:

The *first alteration event* involved the replacement of olivine and pyroxene by serpentine, as well as the desulfurization of primary sulfides and their transformation into alloys. This process was widespread at Agios Iohannis and Northern Agios Iohannis, whereas it was less developed in Agia Alexandria as testified by the lack of Ni-Fe alloys.

The *second alteration event* promoted the alteration of chromite into Fe-chromite, and the formation of chlorite. This stage was widespread at Agia Alexandria, where chlorite is more abundant, probably due to local changes in the oxygen fugacity.

The *third alteration stage* involved the precipitation of Cr-garnet, of the andradite-uvarovite solid solution, formed by reaction of serpentine and Fe-chromite in the presence of aqueous fluids.

Cr-garnets precipitated as coronas surrounding pristine chromite cores, by fully replacing Fe-chromite rims. This stage was detected at Agios Iohannis and Northern Agios Iohannis, while it is absent at Agia Alexandria.

The order in which the alteration events occur in an ophiolite can strongly affect the final mineral assemblage. Cr-garnets can be Fe- or Al-rich based on the magnitude and order of previous alteration stages. In particular, chloritization events lead to loss in Al in the spinel, so the garnet forming reaction will lead towards uvarovite-andradite solid solution products.

ACKNOWLEDGEMENTS

The authors would like to acknowledge the Editorial staff of *Ofioliti* and the reviewers for their constructive comments, which helped to significantly improve the manuscript.

REFERENCES

- Abe N., 2011. Petrology of podiform chromitite from the ocean floor at the 15°20'N FZ in the MAR, Site 1271, ODP Leg 209. *J. Miner. Petrol. Sci.*, 106: 97-102. <https://doi.org/10.2465/jmps.101022>
- Ahmed A.H. and Surour A.A., 2016. Fluid-related modifications of Cr-spinel and olivine from ophiolitic peridotites by contact metamorphism of granitic intrusions in the Ablah area, Saudi Arabia. *J. Asian Earth Sci.*, 122: 58-79. <https://doi.org/10.1016/j.jseaes.2016.03.010>
- Ahmed A.H., Arai S., Abdel-Aziz Y.M., Ikenne M. and Rahimi A., 2009. Platinum-group elements distribution and spinel composition in podiform chromitites and associated rocks from the upper mantle section of the Neoproterozoic Bou Azzer ophiolite, Anti-Atlas, Morocco. *J. Afr. Earth Sci.*, 55: 92-104. <https://doi.org/10.1016/j.jafrearsci.2009.02.005>
- Arai S., 1997. Origin of podiform chromitites. *J. Asian Earth Sci.*, 15: 303-310. [https://doi.org/10.1016/S0743-9547\(97\)00015-9](https://doi.org/10.1016/S0743-9547(97)00015-9)
- Bach W., Paulick H., Garrido C.J., Ildefonse B., Meurer W.P. and Humphris S.E., 2006. Unraveling the sequence of serpentinization reactions: petrography, mineral chemistry, and petrophysics of serpentinites from MAR 15°N (ODP Leg 209, Site 1274). *Geophys. Res. Lett.*, 33. <https://doi.org/10.1029/2006GL025681>
- Ballhaus C., 1998. Origin of podiform chromite deposits by magma mingling. *Earth Planet. Sci. Lett.*, 156: 185-193. [https://doi.org/10.1016/S0012-821X\(98\)00005-3](https://doi.org/10.1016/S0012-821X(98)00005-3)
- Barnes S.J. and Roeder P.L., 2001. The range of spinel compositions in terrestrial mafic and ultramafic rocks. *J. Petrol.*, 42: 2279-2302. <https://doi.org/10.1093/petrology/42.12.2279>
- Beccaluva L., Coltorti M., Prenti I., Saccani E., Siena F. and Zeda O., 1994. Mid-ocean ridge and suprasubduction affinities in the ophiolitic belts from Albania. *Ofioliti*, 19: 77-96.
- Bonev N., Moritz R., Borisova M. and Filipov P., 2019. Thermally-Volvi-Gomati complex of the Serbo-Macedonian Massif, northern Greece: a Middle Triassic continental margin ophiolite of Neotethyan origin. *J. Geol. Soc. London*, 176: 931-944. <https://doi.org/10.1144/jgs2017-130>
- Bortolotti V. and Principi G., 2005. Tethyan ophiolites and Pangea break-up. *Island Arc*, 14: 442-470. <https://doi.org/10.1111/j.1440-1738.2005.00478.x>
- Bortolotti V., Chiari M., Marroni M., Pandolfi L., Principi G. and Saccani E., 2013. Geodynamic evolution of ophiolites from Albania and Greece (Dinaric-Hellenic belt): one, two, or more oceanic basins? *Intern. J. Earth Sci.*, 102: 783-811. <https://doi.org/10.1007/s00531-012-0835-7>
- Boundi D., Papanikolaou D., Bosio G. and Montemagni C., 2024. Late Cretaceous tectono-metamorphic events in the Skyros Upper Metamorphic Unit (Olympus Mountain), Aegean Sea, Greece. *Geosciences (Basel)*, 14: 69. <https://doi.org/10.3390/geosciences14030069>
- Bussolesi M., Grieco G., Cavallo A. and Zaccarini F., 2022a. Different tectonic evolution of fast cooling ophiolite mantles recorded by olivine-spinel geothermometry: case studies from Iballe (Albania) and Nea Roda (Greece). *Minerals*, 12: 64. <https://doi.org/10.3390/min12010064>
- Bussolesi M., Grieco G., Zaccarini F., Cavallo A., Tzamos E. and Storni N., 2022b. Chromite compositional variability and associated PGE enrichments in chromitites from the Gomati and Nea Roda ophiolite, Chalkidiki, Northern Greece. *Miner. Dep.* 57: 1323-1342. <https://doi.org/10.1007/s00126-022-01109-z>
- Bussolesi M., Zaccarini F., Grieco G. and Tzamos E., 2020. Rare and new compounds in the Ni-Cu-Sb-As system: First occurrence in the Gomati ophiolite, Greece. *Per. Miner.*, 89: 63-76. <https://doi.org/10.2451/2020PM893>
- Chakraborty K.L., 1968. Mineralogical note on the chrome-chlorite (kämmererite) and chrome-garnet (uvarovite) from the chromite deposits of Kalrangi, Orissa, India. *Miner. Mag. and J. Miner. Soc.*, 36: 962-965. <https://doi.org/DOI:10.1180/min-mag.1968.283.036.07>
- Chen C., Su B.-X., Xiao Y., Pang K.-N., Robinson P.T., Uysal I., Lin W., Qin K.-Z., Avcı E. and Kapsiotis, A., 2019. Intermediate chromitite in Kızıldağ ophiolite (SE Turkey) formed during subduction initiation in Neo-Tethys. *Ore Geol. Rev.*, 104: 88-100. <https://doi.org/10.1016/j.oregeorev.2018.10.004>
- Chiari M., Bortolotti V., Marcucci M., Photiades A., Principi G. and Saccani E., 2012. Radiolarian biostratigraphy and geochemistry of the Koziakas massif ophiolites (Greece). *Bull. Soc. Géol. Fr.*, 183: 287-306. <https://doi.org/10.2113/gssgfbull.183.4.287>
- Cocomazzi G., Grieco G., Tartarotti P., Bussolesi M., Zaccarini F., Crispini L. and Science Team, O.D.P., 2020. The formation of dunite channels within harzburgite in the Wadi Tayin Massif, Oman Ophiolite: Insights from compositional variability of Cr-Spinel and Olivine in Holes BA1B and BA3A, OD P. *Minerals*, 10: 167. <https://doi.org/10.3390/min10020167>
- Dick H.J.B. and Bullen T., 1984. Chromian spinel as a petrogenetic indicator in abyssal and Alpine-type peridotites and spatially associated lavas. *Contrib. Miner. Petrol.*, 86: 54-76. <https://doi.org/10.1007/BF00373711>
- Dilek Y. and Furnes H., 2014. Ophiolites and Their Origins. *Elements*, 10: 93-100. <https://doi.org/10.2113/gselements.10.2.93>
- Economou-Eliopoulos M., 1996. Platinum-group element distribution in chromite ores from ophiolite complexes: implications for their exploration. *Ore Geol. Rev.*, 11: 363-381. [https://doi.org/10.1016/S0169-1368\(96\)00008-X](https://doi.org/10.1016/S0169-1368(96)00008-X)
- Eslami A., Arai S., Miura M. and Mackizadeh M.A., 2018. Metallogeny of the peridotite-hosted magnetite ores of the Nain ophiolite, Central Iran: Implications for Fe concentration processes during multi-episodic serpentinization. *Ore Geol. Rev.*, 95: 680-694. <https://doi.org/10.1016/j.oregeorev.2018.03.020>
- Ferrière J., Chanier F. and Ditbanjong P., 2012. The Hellenic ophiolites: eastward or westward obduction of the Maliaic Ocean, a discussion. *Intern. J. Earth Sci.*, 101: 1559-1580. <https://doi.org/10.1007/s00531-012-0797-9>
- Frost B.R., 1985. On the stability of sulfides, oxides, and native metals in serpentinite. *J. Petrol.*, 26: 31-63. <https://doi.org/10.1093/petrology/26.1.31>
- Frost B.R. and Beard J.S., 2007. On Silica Activity and Serpentinization. *J. Petrol.*, 48: 1351-1368. <https://doi.org/10.1093/petrology/egm021>
- Ghosh B. and Morishita T., 2011. Andradite-Uvarovite solid solution from hydrothermally altered podiform chromitite, Rutland Ophiolite, Andaman, India. *Can. Miner.*, 49: 573-580. <https://doi.org/10.3749/canmin.49.2.573>
- González-Jiménez J.M., Griffin W.L., Proenza J.A., Gervilla F., O'Reilly S.Y., Akbulut M., Pearson N.J. and Arai S., 2014. Chromitites in ophiolites: How, where, when, why? Part II. The crystallization of chromitites. *Lithos*, 189: 140-158. <https://doi.org/10.1016/j.lithos.2013.09.008>
- Grammatikopoulou, T.A., Kapsiotis, A., Tsikouras B., Hatzipanagiotou K., Zaccarini F. and Garuti G., 2011. Spinel composition, pge geochemistry and mineralogy of the chromitites from the Vourinos Ophiolite Complex, Northwestern Greece. *Can. Miner.*, 49: 1571-1598. <https://doi.org/10.3749/canmin.49.6.1571>
- Grieco G. and Merlini A., 2012. Chromite alteration processes within Vourinos ophiolite. *Intern. J. Earth Sci.*, 101: 1523-1533. <https://doi.org/10.1007/s00531-011-0693-8>
- Grieco G., Bussolesi M., Eslami A., Gentile A., Cavallo A., Lian D., Yang J. and Ghaseminejad F., 2020. Differential platinum group elements (PGE) re-mobilization at low fS₂ in Abdasht and Soghan mafic-ultramafic complexes (Southern Iran). *Lithos*, 366-367: 105523. <https://doi.org/10.1016/j.lithos.2020.105523>

- Grieco G., Bussolesi M., Tzamos E., Rassios A.E. and Kapsiotis A., 2018. Processes of primary and re-equilibration mineralization affecting chromitite ore geochemistry within the Vourinos ultramafic sequence, Vourinos ophiolite (West Macedonia, Greece). *Ore Geol. Rev.*, 95: 537-551.
- Grieco G., Cavallo A., Maescotti P., Crispini L., Maescotti P., Tzamos E. and Bussolesi M., 2023. The formation of magnesite ores by reactivation of dunite channels as a key to their spatial association to chromite ores in ophiolites: An example from Northern Evia, Greece- Minerals, 13. <https://doi.org/https://doi.org/10.3390/min13020159>
- Grieco G., Pedrotti M. and Moroni M., 2011. Metamorphic redistribution of Cr within chromitites and its influence on chromite ore enrichment. *Miner. Eng.*, 24: 102-107.
- Harder H., Jacobshagen V., Skala W., Arafah M., Berndsen J., Hofmann A., Kusserow H. and Schedler W., 1983. Geologische Entwicklung und Struktur der Insel Skyros, Nordsporaden, Griechenland. *Berl. Geowiss. Abhandl.*, 48: 7-40.
- Kapsiotis A., Rassios A.E., Uysal I., Grieco G., Akmaz R.M., Saka S. and Bussolesi M., 2018. Compositional fingerprints of chromian spinel from the refractory chrome ores of Metalleion, Othris (Greece): Implications for metallogeny and deformation of chromitites within a "hot" oceanic fault zone. *J. Geochem. Explor.*, 185: 14-32. <https://doi.org/https://doi.org/10.1016/j.gexplo.2017.11.003>
- Karkalis C., Magganas A. and Koutsovitis P., 2017. Petrological, mineralogical and geochemical data from the Eohellenic Ophiolitic Nappe in the island of Skyros, Greece. *Bull. Géol. Soc. Gr.*, 50: 1867. <https://doi.org/10.12681/bgs.11926>
- Kilias A.A., Frisch W., Avgerinas A., Dunkl I., Falalakis G. and Gawlick H., 2010. Alpine architecture and kinematics of deformation of the northern Pelagonian nappe pile in the Hellenides. *Austr. J. Earth Sci.*, 103: 4-28.
- Liu R., Zhao J., Zhou M. and Qi H., 2023. Alteration of chromite during serpentinization of peridotites. *Lithos*, 460-461, 107385. <https://doi.org/10.1016/j.lithos.2023.107385>
- McDonough W.F. and Sun S.-S., 1995. The composition of the Earth. *Chem. Geol.*, 120: 223-253. [https://doi.org/10.1016/0009-2541\(94\)00140-4](https://doi.org/10.1016/0009-2541(94)00140-4)
- Melcher, Frank, Grum, W., Simon G., Thalhammer T.V. and Stumpf E.F., 1997. Petrogenesis of the ophiolitic giant chromite deposits of Kempirsai, Kazakhstan: a study of solid and fluid inclusions in chromite. *J. Petrol.*, 38: 1419-1458. <https://doi.org/10.1093/ptro/38.10.1419>
- Melcher F., Grum W., Simon G., Thalhammer T.V. and Stumpf E.F., 1997. Petrogenesis of the ophiolitic giant chromite deposits of Kempirsai, Kazakhstan: a study of solid and fluid inclusions in chromite. *J. Petrol.*, 38: 1419-1458. <https://doi.org/10.1093/ptro/38.10.1419>
- Mellini M., Rumori C. and Viti C., 2005. Hydrothermally reset magmatic spinels in retrograde serpentinites: formation of "ferritchromite" rims and chlorite aureoles. *Contrib. Miner. Petrol.*, 149: 266-275. <https://doi.org/10.1007/s00410-005-0654-y>
- Merlini A., Giovanni G. and Valeria D., 2009. Ferritchromite and chromian-chlorite formation in mélange-hosted Kalkan chromitite (Southern Urals, Russia). *Am. Miner.*, 94: 1459-1467. <https://doi.org/10.2138/am.2009.3082>
- Miura M., Arai S., Ahmed A.H., Mizukami T., Okuno M. and Yamamoto S., 2012. Podiform chromitite classification revisited: A comparison of discordant and concordant chromitite pods from Wadi Hilti, northern Oman ophiolite. *J. Asian Earth Sci.*, 59: 52-61. <https://doi.org/10.1016/j.jseas.2012.05.008>
- Pal T. and Das D., 2010. Uvarovite from chromite-bearing ultramafic intrusives, Orissa, India, a crystal-chemical characterization using 57Fe Mössbauer spectroscopy. *Am. Miner.*, 95: 839-843. <https://doi.org/https://doi.org/10.2138/am.2010.3328>
- Papantoniou, G., 2015. The structure and history of the strike-slip fault Zone of Skyros Island, Central-North Aegean. National and Kapodistrian University of Athens, Athens.
- Paraskevopoulos G.M. and Economou M., 1981. Zoned Mn-rich chromite from podiform type chromite ore in serpentinites of northern Greece. *Am. Miner.*, 66: 1013-1019.
- Pe-Piper G., and Piper D.J.W., 2002. The igneous rocks of Greece. The anatomy of an orogeny.
- Proenza J., Sole J. and Melgarejo J.C., 1999. Uvarovite in podiform chromitite; the Moa-Baracoa ophiolitic massif, Cuba. *Can. Miner.*, 37: 679-690.
- Proenza J.A., Zaccarini F., Lewis J.F., Long F. and Garuti G., 2007. Chromian spinel composition and the Platinum-Group Minerals of the PGE-rich Loma Peguera Chromitites, Loma Caribe Peridotite, Dominican Republic. *Can. Miner.*, 45: 631-648. <https://doi.org/10.2113/gscanmin.45.3.631>
- Qiu T., Yang J., Milushi I., Wu W., Mekshiqi N., Xiong F., Zhang C. and Shen T., 2018. Petrology and PGE Abundances of High-Cr and High-Al Podiform Chromitites and Peridotites from the Bulqiza Ultramafic Massif, Eastern Mirdita Ophiolite, Albania. *Acta Geol. Sin. Engl. Ed.*, 92: 1063-1081. <https://doi.org/10.1111/1755-6724.13592>
- Rassios A.E. and Dilek Y., 2009. Rotational deformation in the Jurassic Mesohellenic ophiolites, Greece, and its tectonic significance. *Lithos*, 108: 207-223. <https://doi.org/10.1016/j.lithos.2008.09.005>
- Robertson A.H.F., Dixon J.E., Brown S., Collins A., Morris A., Pickett E., Sharp I. and Ustaömer T., 1996. Alternative tectonic models for the Late Palaeozoic-Early Tertiary development of Tethys in the Eastern Mediterranean region. *Geol. Soc. London Spec. Publ.*, 105: 239-263. <https://doi.org/10.1144/GSL.SP.1996.105.01.22>
- Saccani E. and Photiades A., 2005. Petrogenesis and tectonomagmatic significance of volcanic and subvolcanic rocks in the Albanide-Hellenide ophiolitic mélanges. *Island Arc*, 14: 494-516. <https://doi.org/10.1111/j.1440-1738.2005.00480.x>
- Saccani E. and Tassinari R., 2015. The role of MORB and SSZ magma-types in the formation of Jurassic ultramafic cumulates in the Mirdita ophiolites (Albania) as deduced from chromian spinel and olivine chemistry. *Ophioliti*, 40: 37-56.
- Saccani E., Beccaluva L., Photiades A. and Zeda O., 2011. Petrogenesis and tectono-magmatic significance of basalts and mantle peridotites from the Albanian-Greek ophiolites and sub-ophiolitic mélanges. New constraints for the Triassic-Jurassic evolution of the Neo-Tethys in the Dinaride sector. *Lithos*, 124: 227-242. <https://doi.org/10.1016/j.lithos.2010.10.009>
- Saccani E., Chiari M., Bortolotti V., Photiades A. and Principi G., 2015. Geochemistry of volcanic and subvolcanic rocks and biostratigraphy on radiolarian cherts from the Almopias Ophiolites and Paikon Unit (Western Vardar, Greece). *Ophioliti*, 40: 1-25.
- Saccani E., Dilek Y. and Photiades A., 2017. Time-progressive mantle-melt evolution and magma production in a Tethyan marginal sea: A case study of the Albanide-Hellenide ophiolites. *Lithosphere*, 10: 35-53. <https://doi.org/10.1130/L602.1>
- Saccani E., Photiades A., Santato A. and Zeda O., 2008. New Evidence for Supra-Subduction Zone Ophiolites in the Vardar Zone of Northern Greece: Implications for the tectono-magmatic evolution of the Vardar Oceanic Basin. *Ophioliti*, 33: 65-85.
- Saumur B.M. and Hattori K., 2013. Zoned Cr-spinel and ferritchromite alteration in forearc mantle serpentinites of the Rio San Juan Complex, Dominican Republic. *Mineral. Mag.*, 77: 117-136. <https://doi.org/10.1180/minmag.2013.077.1.11>
- Schmid S.M., Bernoulli D., Fügenschuh B., Matenco L., Schefer S., Schuster R., Tischler M. and Ustaszewski K., 2008. The Alpine-Carpathian-Dinaridic orogenic system: correlation and evolution of tectonic units. *Swiss J. Geosci.*, 101: 139-183. <https://doi.org/10.1007/s00015-008-1247-3>
- Schulte R.F. and Pack A., 2024. Mineral Industry Surveys.
- Sideridis A., Tsikouras B., Tsitsanis P., Koutsovitis P., Zaccarini F., Hauzenberger C., Tsikos H. and Hatzipanagiotou K., 2022. Post-magmatic processes recorded in bimodal chromitites of the East Chalkidiki meta-ultramafic bodies, Gomati and Nea Roda, Northern Greece. *Front. Earth Sci., Lausanne*, 10. <https://doi.org/10.3389/feart.2022.1031239>
- Sideridis A., Zaccarini F., Koutsovitis P., Grammatikopoulos T., Tsikouras B., Garuti G. and Hatzipanagiotou K., 2021. Chromitites from the Vavdos ophiolite (Chalkidiki, Greece): Pet-

- rogenesis and geotectonic settings; constrains from spinel, olivine composition, PGE mineralogy and geochemistry. *Ore Geol. Rev.*, 137. <https://doi.org/https://doi.org/10.1016/j.oregeorev.2021.104289>
- Spiegelman M. and Kelemen P.B., 2003. Extreme chemical variability as a consequence of channelized melt transport. *Geochem. Geophys. Geosyst.*, 4. <https://doi.org/10.1029/2002GC000336>
- Tarkian M., Economou-Eliopoulos M. and Eliopoulos D.G., 1992. Platinum-group minerals and tetraauricupride in ophiolitic rocks of Skyros island, Greece. *Miner. Petrol.*, 47: 55-66. <https://doi.org/10.1007/BF01165297>
- Tsoupas G. and Economou-Eliopoulos M., 2008. High PGE contents and extremely abundant PGE-minerals hosted in chromitites from the Veria ophiolite complex, northern Greece. *Ore Geol. Rev.*, 33: 3-19. <https://doi.org/10.1016/j.oregeorev.2006.10.008>
- Uysal I., Akmaz.M., Saka S. and Kapsiotis A., 2016. Coexistence of compositionally heterogeneous chromitites in the Antalya-Isparta ophiolitic suite, SW Turkey: A record of sequential magmatic processes in the sub-arc lithospheric mantle. *Lithos*, 248-251: 160-174. <https://doi.org/10.1016/j.lithos.2016.01.021>
- Uysal İ., Tarkian M., Sadiklar M.B., Zaccarini F., Meisel T., Garuti G. and Heidrich S., 2009. Petrology of Al- and Cr-rich ophiolitic chromitites from the Muğla, SW Turkey: implications from composition of chromite, solid inclusions of platinum-group mineral, silicate, and base-metal mineral, and Os-isotope geochemistry. *Contrib. Miner. Petrol.*, 158: 659-674. <https://doi.org/10.1007/s00410-009-0402-9>
- Xiong F., Yang J., Robinson P.T., Xu X., Liu Z., Zhou W., Feng G., Xu J., Li J. and Niu X., 2017. High-Al and high-Cr podiform chromitites from the western Yarlung-Zangbo suture zone, Tibet: Implications from mineralogy and geochemistry of chromian spinel, and platinum-group elements. *Ore Geol. Rev.*, 80: 1020-1041. <https://doi.org/10.1016/j.oregeorev.2016.09.009>
- Zaccarini F., Proenza J.A., Ortega-Gutiérrez F. and Garuti G., 2005. Platinum group minerals in ophiolitic chromitites from Tehuiztingo (Acatlán complex, southern Mexico): implications for post-magmatic modification. *Miner. Petrol.*, 84: 147-168. <https://doi.org/10.1007/s00710-005-0075-7>
- Zachariadis P.T., 2007. Ophiolites of the eastern Vardar zone, N. Greece. University of Mainz, Germany.
- Zhou M.-F. and Robinson P.T., 1994. High-Cr and High-Al Podiform Chromitites, Western China: Relationship to Partial Melting and Melt/Rock Reaction in the Upper Mantle. *Intern. Geol. Rev.*, 36: 678-686. <https://doi.org/10.1080/00206819409465481>
- Zhou M.-F., Robinson P.T., Malpas J., Aitchison J., Sun M., Bai W.-J., Hu X.-F. and Yang J.-S., 2001. Melt/mantle interaction and melt evolution in the Sartohay high-Al chromite deposits of the Dalabute ophiolite (NW China). *J. Asian Earth Sci.*, 19: 517-534. [https://doi.org/10.1016/S1367-9120\(00\)00048-1](https://doi.org/10.1016/S1367-9120(00)00048-1)
- Zhou M.-F., Robinson P.T., Malpas J. and Li Z., 1996. Podiform chromitites in the Luobusa Ophiolite (Southern Tibet): Implications for melt-rock interaction and chromite segregation in the upper mantle. *J. Petrol.*, 37: 3-21. <https://doi.org/10.1093/petrology/37.1.3>

Received, October 9, 2024
Accepted, November 26, 2024